Particle-vibration coupling within covariant density functional theory

E. Litvinova

*Physik-Department der Technischen Universität München, D-85748 Garching, Germany and
Institute of Physics and Power Engineering, RU-249033 Obninsk, Russia*

P. Ring

Physik-Department der Technischen Universität München, D-85748 Garching, Germany

V. Tselyaev

Nuclear Physics Department, V.A. Fock Institute of Physics, St. Petersburg State University, RU-198504 St. Petersburg, Russia

Covariant density functional theory, which has so far been applied only within the framework of static and time-dependent mean-field theory, is extended to include particle-vibration coupling (PVC) in a consistent way. Starting from a conventional energy functional, we calculate the low-lying collective vibrations in the relativistic random phase approximation (RRPA) and construct an energy-dependent self-energy for the Dyson equation. The resulting Bethe-Salpeter equation in the particle-hole (p-h) channel is solved in the time blocking approximation (TBA). No additional parameters are used, and double counting is avoided by a proper subtraction method. The same energy functional, i.e., the same set of coupling constants, generates the Dirac-Hartree single-particle spectrum, the static part of the residual p-h interaction, and the particle-phonon coupling vertices. Therefore, a fully consistent description of nuclear excited states is developed. This method is applied for an investigation of damping phenomena in the spherical nuclei with closed shells ^{208}Pb and ^{132}Sn. Since the phonon coupling terms enrich the RRPA spectrum with a multitude of p-h⊗phonon components, a noticeable fragmentation of the giant resonances is found, which is in full agreement with experimental data and with results of the semiphenomenological nonrelativistic approach.

I. INTRODUCTION

The theoretical analysis of nuclear dynamics by microscopic methods remains undoubtedly a crucial issue of present-day nuclear physics. Besides the merely theoretical interest, it is stimulated by new experimental opportunities for the study of the nuclear many-body system. Along with new possibilities to investigate more precisely nuclear systems being considered well known, the recent generation of radioactive-beam facilities enables us to examine exotic systems with extreme spin and isospin values. For a successful description of nuclei close to the limits of stability, a powerful and reliable theory should be provided. It should be based on a consistent treatment of both ground and excited states, and it should allow predictions of nuclear properties in areas which are hard or impossible to access by future experiments.

Ab initio calculations and multiconfiguration mixing within the shell model can, so far, only be applied to light nuclei. At present, for a universal description of nuclei over the entire periodic table, density functional theory (DFT) based on the mean-field concept provides a very reasonable approach. DFT was introduced in the 1960s in atomic and molecular physics [1,2] and shortly after that in nuclear physics, where it has been called the density-dependent Hartree-Fock theory [3,4]. Today it is widely used on all kinds of quantum mechanical many-body systems. Density functional theory can, in principle, provide an exact description of the many-body dynamics, if the exact density functional is known; but for such systems as nuclei, one is far from a microscopic derivation and one is forced to determine the functional in a phenomenological way. Starting from basic symmetries, the parameters are adjusted to characteristic experimental data in finite nuclei and nuclear matter.

One of the most successful schemes of this type is covariant density functional theory (CDFT). It is based on Lorentz invariance, connecting in a consistent way the spin and spatial degrees of freedom in the nucleus. Therefore, it needs only a relatively small number of parameters which are adjusted to reproduce a set of bulk properties of spherical closed-shell nuclei [5,6]. A large variety of nuclear phenomena have been described over the years within this kind of model: ground state properties of finite spherical and deformed nuclei over the entire periodic table [7] from light nuclei [8] to super-heavy elements [9,10], from the neutron drip line, where halo phenomena are observed [11], to the proton drip line [12] with nuclei unstable against the emission of protons [13]. Rotational bands are treated within the relativistic cranking approximation [14,15], and the relativistic random phase approximation (RRPA) [16] and quasiparticle RRPA [17] have been formulated as the small amplitude limit of time-dependent relativistic mean-field (RMF) models for a description of collective and noncollective excitations. This method is successful, in particular, in describing the positions of giant resonances and spin/isospin excitations such as the isobaric analog resonance (IAR) or the Gamow-Teller resonance (GTR) [18]. Recently, it was also used for a theoretical interpretation of low-lying dipole [17] and quadrupole [19] excitations.

With a few exceptions, where the quadrupole motion has been studied within the relativistic generator coordinate method (GCM) [20], applications of CDFT to the description of excited states are limited to the relativistic RPA, i.e., to configurations of a one-particle one-hole (1p-1h) nature. None of these methods, however, can be applied to the investigation of a coupling to more complicated configurations as occurs, for instance, in the damping phenomena causing the width of giant resonances. It is also known that in such theories, because of the low values of the effective mass, the level density of the single-particle spectrum in the vicinity of the Fermi surface is considerably reduced as compared with experimental data.

Based on the Fermi liquid theory (FLT) of Landau [21], the theory of finite Fermi systems (TFFS) of Migdal [22] is another very successful method for describing low-lying nuclear excitations [23], which has been known since the 1950s. It has several general properties in common with density functional theory. First, both theories are known to be exact, at least in principle, but in practice the parameters entering these theories have to be determined in a phenomenological way by adjustment to experimental data. Second, both theories are based in some sense on a single-particle concept. DFT uses the mean-field concept with Slater determinants in an effective single-particle potential as a vehicle to introduce shell effects in an exact theory, and FLT is based on the concept of quasiparticles obeying a Dyson equation, which are defined as the basic excitations of the neighboring system with odd particle number. Third, in practical applications both theories describe in the simplest versions the nuclear excitations in the RPA approximation, i.e., by a linear combination of particle-hole (p-h) configurations in an average nuclear potential.

However, there are also essential differences between these two concepts. First, in contrast to DFT, TFFS does not attempt to calculate the ground state properties of the many-body system, but it describes the nuclear excitations in terms of Landau quasiparticles and their interaction. Therefore, the experimental data used to fix the phenomenological parameters of the theories are bulk properties of the ground state in the case of density functional theory, and properties of single-particle excitations and of the collective excitations in the case of finite Fermi systems theory. Second, DFT determines the mean field in a self-consistent way, and therefore the RPA spectrum contains Goldstone modes at zero energy. This is usually not the case in TFFS calculations, which are based on a nonrelativistic shell-model potential, whose parameters are adjusted to the experimental single-particle spectra. Therefore there is no self-consistency in the RPA calculations of TFFS, and the Goldstone modes are not separated from the other modes. They are distributed among the low-lying excitations. Third, modern versions of TFFS go much beyond the mean-field approximation. Green's function techniques have been used to investigate the coupling between quasiparticles and phonons. Based on the phonons calculated in the framework of the RPA, one has included particle-phonon coupling vertices and an energy dependence of the self-energy in the Dyson equation [24,25]. This leads also to an induced interaction in the Bethe-Salpeter equation caused by the exchange of phonons which also depends on the energy. The coupling of particles and phonons has also been derived

from nuclear field theory (NFT) and its extensions [26–28]. Many aspects of the coupling between the quasiparticles and the collective vibrations have been investigated with these techniques [29–38] as well as with other kinds of approaches beyond RPA [39,40] over the years.

The present work attempts to find a combination of the basic ideas of density functional theory and Landau-Migdal theory. The concept is similar to that applied in earlier work [41–43], which used specific nonrelativistic energy functionals to construct self-consistent TFFS. We start here from a covariant density functional $E[\rho]$ widely used in the literature. It is adjusted to ground state properties of characteristic nuclei, and, without any additional parameters, it provides the necessary input of finite Fermi systems theory, such as the mean field and the single-particle spectrum as well as an effective interaction between the p-h configurations in terms of the second derivative of the same energy $E[\rho]$ with respect to the density. Thus the phenomenological input of Landau-Migdal theory is replaced by the results of density functional theory. The same interaction is used to calculate the vertices for particle-vibration coupling [44]. We then apply the techniques of Landau-Migdal theory and its modern extensions to describe vibrational coupling and complex configurations. In this way, we obtain a fully consistent description of the many-body dynamics.

Two essential approximations are used in this context. First, the *time-blocking approximation* (TBA) blocks in a special time-projection technique the 1p-1h propagation through states which have a more complex structure than 1p1h⊗phonon. The nuclear response can then be explicitly calculated on the 1p1h+1p1h⊗phonon level by summation of an infinite series of Feynman's diagrams. This approximation has been introduced in Ref. [34]. Initially it was called the method of chronological decoupling of diagrams (MCDD), and it is also discussed in recent review articles [35,36]. Second, a special *subtraction technique* guarantees that there is no double counting between the additional correlations introduced by particle-vibration coupling and the ground state correlations already taken into account in the phenomenological density functional. These two tools are essential for the success of the present method. TBA introduces a consistent truncation scheme into the Bethe-Salpeter equation, and without it it would be hard to solve the equations explicitly. The subtraction method is the essential tool for connecting density functional theory, so far used only on the level of mean field theory, i.e., on the RPA level, with the extended Landau-Migdal theory, where complex configurations are included through particle-vibration coupling.

As discussed above, there are several versions of DFT in nuclear system. In the present work, we use CDFT with the parameter set NL3 [45]. A first attempt in this direction has been carried out in Ref. [44], where we treated the level density problem in the framework of covariant particle-vibration coupling.

In Sec. II, we discuss briefly the general CDFT formalism, we introduce the concept of the energy-dependent self-energy $\Sigma(\varepsilon)$ and the vertices of particle-vibration coupling in the relativistic framework, and we discuss the response formalism and time blocking approximation for the response function. In

Sec. III, we show how to solve the resulting integral equations in detail and present recent numerical applications for the spreading width of the doubly magic nuclei ^{208}Pb and ^{132}Sn; in Sec. IV, we include a brief summary and an outlook for future applications. Appendices A–D provide more details on the formalism used in the calculations.

II. FORMALISM

A. Relativistic mean-field approach

In relativistic mean-field theory, the nucleus is considered to be a system of nucleons interacting by the exchange of effective mesons, which characterize the quantum numbers of the various fields. Conventional RMF theory uses σ, ω, and ρ mesons and the photon as the minimal set of bosons necessary to generate realistic nuclear fields [5,46,47]. This concept is expressed by the following Lagrangian density depending on the nucleon spinor ψ as well as on the mesons σ, ω^{μ}, $\vec{\rho}^{\mu}$, and the electromagnetic fields A^{μ}:

$$
\begin{aligned}
\mathcal{L} = {} & \bar{\psi}(i\gamma^{\mu}\partial_{\mu} - m)\psi + \tfrac{1}{2}\partial^{\mu}\sigma\,\partial_{\mu}\sigma - \tfrac{1}{2}m_{\sigma}^{2}\sigma^{2} - \tfrac{1}{4}\Omega^{\mu\nu}\Omega_{\mu\nu} \\
& + \tfrac{1}{2}m_{\omega}^{2}\omega^{\mu}\omega_{\mu} - \tfrac{1}{4}\vec{R}^{\mu\nu}\vec{R}_{\mu\nu} + \tfrac{1}{2}m_{\rho}^{2}\vec{\rho}^{\mu}\vec{\rho}_{\mu} - \tfrac{1}{4}F^{\mu\nu}F_{\mu\nu} \\
& - \bar{\psi}\big(\Gamma_{\sigma}\sigma + \Gamma_{\omega}^{\mu}\omega_{\mu} + \vec{\Gamma}_{\rho}^{\mu}\vec{\rho}_{\mu} + \Gamma_{e}^{\mu}A_{\mu}\big)\psi.
\end{aligned} \tag{1}
$$

Here m is the bare nucleon mass, m_{σ}, m_{ω}, and m_{ρ} are the corresponding meson masses, and $\Omega_{\mu\nu}$, $\vec{R}_{\mu\nu}$, $F_{\mu\nu}$ are the field tensors

$$
\begin{aligned}
\Omega_{\mu\nu} &= \partial_{\mu}\omega_{\nu} - \partial_{\nu}\omega_{\mu}, \\
\vec{R}_{\mu\nu} &= \partial_{\mu}\vec{\rho}_{\nu} - \partial_{\nu}\vec{\rho}_{\mu}, \\
F_{\mu\nu} &= \partial_{\mu}A_{\nu} - \partial_{\nu}A_{\mu}.
\end{aligned} \tag{2}
$$

As usual, arrows denote isovectors and boldface symbols will be used for vectors in ordinary space. The vertices Γ entering the interaction term of Eq. (1) read

$$
\begin{aligned}
\Gamma_{\sigma} &= g_{\sigma}, \quad \Gamma_{\omega}^{\mu} = g_{\omega}\gamma^{\mu}, \quad \vec{\Gamma}_{\rho}^{\mu} = g_{\rho}\vec{\tau}\gamma^{\mu}, \\
\Gamma_{e}^{\mu} &= e\frac{(1-\tau_{3})}{2}\gamma^{\mu},
\end{aligned} \tag{3}
$$

where g_{σ}, g_{ω}, g_{ρ}, and e are the corresponding coupling constants. For the sake of simplicity, we use in the following discussions the linear version (1) of the Lagrangian. However, it is well known that one needs an additional density dependence in order to obtain a reliable description of nuclear surface properties. It is either expressed by a nonlinear self-interaction between the mesons or by an explicit density dependence of the coupling constants g_{σ}, g_{ω}, and g_{ρ}. In all the numerical applications, we use such modifications, which are discussed in detail in Appendix A.

The classical variation principle being applied to the Lagrangian density (1) leads to a system of coupled equations of motion for the fermions

$$
\left(i\gamma^{\mu}\partial_{\mu} - m - \sum_{m}\Gamma_{m}\phi_{m}(\mathbf{r},t)\right)\psi_{i}(\mathbf{r},t) = 0, \tag{4}
$$

and the mesons

$$
\big(\Box + m_{m}^{2}\big)\phi_{m}(\mathbf{r},t) = \mp\sum_{i}\bar{\psi}_{i}(\mathbf{r},t)\Gamma_{m}\psi_{i}(\mathbf{r},t). \tag{5}
$$

Here the index i numerates the nucleons, and the index $m = \{\sigma, \omega, \rho, e\}$ runs over the set of meson fields $\phi_{m} = \{\sigma, \omega^{\mu}, \vec{\rho}^{\mu}, A^{\mu}\}$. m_{m} are the corresponding masses and Γ_{m} are the vertices (3). The minus sign in Eq. (5) holds for scalar fields, and the plus sign for vector fields. The set of Eqs. (4) and (5) defines the standard RMF model, which implies the following four approximations:

(i) Only the motion of the nucleons is quantized; the meson and electromagnetic degrees of freedom are described by *classical fields*. The nucleons move independently in these classical fields; i.e., residual two-body correlations are disregarded and the many-nucleon wave function is a Slater determinant at all times.

(ii) In time-dependent applications, we use the *instantaneous approximation*, i.e., the time derivatives ∂_{t}^{2} in the Klein-Gordon equations and, consequently, the retardation effects for the meson fields are neglected, although the Dirac spinors ψ_{i} as well as the fields ϕ_{m} are functions of coordinates and time. This is justified by the relatively large meson masses and the corresponding short range of the meson exchange interaction.

(iii) *Fock terms* are neglected. Because of the short-range character of the meson exchange forces, they behave similar to zero range forces, where the Fock terms have the same form as the direct terms and contribute only in a change of the relevant strength parameters. Since our strength parameters are adjusted to experimental data, Fock terms for the heavy mesons are implicitly taken into account to a large extent.

(iv) The *no-sea approximation* means that nucleon states in the Dirac sea with negative energies do not contribute to the densities and currents: the sum over i in Eq. (5) includes only occupied levels with positive energy in the Fermi sea. This means we do not consider vacuum polarization explicitly. Since our parameters are adjusted to experimental data, such effects are taken into account in an implicit way.

B. Energy-dependent nucleon self-energy

Let us now consider in detail the Dyson equation, which describes the motion of a single nucleon in the nuclear interior as

$$
(i\gamma^{\mu}\partial_{\mu} - m - \Sigma)\psi_{i} = 0. \tag{6}
$$

Here the total self-energy Σ contains all the forces acting on the nucleon. As long as one stays within the RMF approach, the nucleon self-energy contains only static and local contributions from the mesons and from the electromagnetic fields.

When we go beyond the mean-field approximation, we have to take into account that in the general case the full self-energy Σ is nonlocal in the space coordinates as well as in time. This nonlocality means that its Fourier transform has both

momentum and energy dependence. Let us now decompose the total self-energy matrix into two components, a static local and an energy-dependent nonlocal term:

$$\Sigma(\mathbf{r}, \mathbf{r}'; \varepsilon) = \tilde{\Sigma}(\mathbf{r})\delta(\mathbf{r} - \mathbf{r}') + \Sigma^e(\mathbf{r}, \mathbf{r}'; \varepsilon), \quad (7)$$

where

$$\tilde{\Sigma}(\mathbf{r}) = \sum_m \Gamma_m \phi_m(\mathbf{r}) \quad (8)$$

is the static part known from RMF theory in Eq. (4). The upper index e in Σ^e indicates the energy dependence. The Dyson equation for single-particle Green's function reads

$$(\varepsilon - h^{\mathcal{D}} - \beta \Sigma^e(\varepsilon))G(\varepsilon) = \beta, \quad (9)$$

where $h^{\mathcal{D}}$ denotes the Dirac Hamiltonian in Eq. (4), with the energy-independent mean field

$$h^{\mathcal{D}} = \boldsymbol{\alpha}\mathbf{p} + \beta(m + \tilde{\Sigma}_s) + \tilde{\Sigma}_0, \quad \boldsymbol{\alpha} = \beta\boldsymbol{\gamma}, \quad \beta = \gamma^0. \quad (10)$$

Most of the static calculations are done for cases where time-reversal symmetry is valid. In all these cases, there are no currents in the nucleus and, thus, only scalar $\tilde{\Sigma}_s$ and time-like $\tilde{\Sigma}_0$ components of $\tilde{\Sigma}$ survive in the static Dirac Hamiltonian of Eq. (10). In the shell-model Dirac basis $\{|\psi_k\rangle\}$, which diagonalizes the energy-independent part of the Dirac equation

$$h^{\mathcal{D}}|\psi_k\rangle = \varepsilon_k|\psi_k\rangle, \quad (11)$$

one can rewrite Eq. (9) as

$$\sum_l \{(\varepsilon - \varepsilon_k)\delta_{kl} - \Sigma^e_{kl}(\varepsilon)\}G_{lk'}(\varepsilon) = \delta_{kk'}, \quad (12)$$

where

$$\Sigma^e_{kl}(\varepsilon) = \int d^3r\, d^3r'\, \bar{\psi}_k(\mathbf{r})\Sigma^e(\mathbf{r}, \mathbf{r}'; \varepsilon)\psi_l(\mathbf{r}'), \quad (13)$$

$$G_{kl}(\varepsilon) = \int d^3r\, d^3r'\, \bar{\psi}_k(\mathbf{r})\beta G(\mathbf{r}, \mathbf{r}'; \varepsilon)\beta\psi_l(\mathbf{r}'). \quad (14)$$

The letter indices k, k', l denote full sets of the single-particle quantum numbers. In the present work, we consider spherical symmetry, so the spinor $|\psi_k\rangle$ is characterized by the set $k = \{(k), m_k\}$ and $(k) = \{n_k, j_k, \pi_k, \tau_k\}$ with the radial quantum number n_k, angular momentum quantum numbers

j_k, m_k, parity π_k, and isospin τ_k, that is,

$$\psi_k(\mathbf{r}, s, t) = \begin{pmatrix} f_{(k)}(r)\Phi_{l_k j_k m_k}(\vartheta, \varphi, s) \\ i g_{(k)}(r)\Phi_{\tilde{l}_k j_k m_k}(\vartheta, \varphi, s) \end{pmatrix} \chi_{\tau_k}(t), \quad (15)$$

where s and t are the coordinates for spin and isospin. The orbital angular momenta l_k and $\tilde{l}_k$ of the large and small components are determined by the parity of the state k, that is,

$$\begin{cases} l_k = j_k + \frac{1}{2}, \, \tilde{l}_k = j_k - \frac{1}{2} & \text{for} \quad \pi_k = (-1)^{j_k + \frac{1}{2}} \\ l_k = j_k - \frac{1}{2}, \, \tilde{l}_k = j_k + \frac{1}{2} & \text{for} \quad \pi_k = (-1)^{j_k - \frac{1}{2}}, \end{cases} \quad (16)$$

$f_{(k)}(r)$ and $g_{(k)}(r)$ are radial wave functions, and $\Phi_{ljm}(\vartheta, \varphi, s)$ is a two-dimensional spinor

$$\Phi_{ljm}(\vartheta, \varphi, s) = \sum_{m_s m_l} \left(\frac{1}{2} m_s l m_l | jm \right) Y_{lm_l}(\vartheta, \varphi)\chi_{m_s}(s). \quad (17)$$

As in Ref. [44], we use the particle-phonon coupling model for the energy-dependent part of the self-energy $\Sigma^e(\varepsilon)$. In the Dirac basis of the spinors $|\psi_k\rangle$ defined in Eq. (11), it has the form

$$\Sigma^e_{kl}(\varepsilon) = \sum_{\mu, n} \frac{\gamma^{\mu(\sigma_n)}_{kn} \gamma^{\mu(\sigma_n)*}_{ln}}{\varepsilon - \varepsilon_n - \sigma_n(\Omega^\mu - i\eta)}, \quad (18)$$

$$\gamma^{\mu(\sigma)}_{kn} = \delta_{\sigma,+1}\gamma^\mu_{kn} + \delta_{\sigma,-1}\gamma^{\mu*}_{nk},$$

where $\eta \to +0$. In Fig. 1, we show a graphical representation of $\Sigma^e_{kl}(\varepsilon)$. The index n runs over all single-particle states in this basis. We distinguish occupied states in the Fermi sea $|h\rangle$ (hole states) with $\sigma_h = -1$, unoccupied states above the Fermi level $|p\rangle$ (particle states) with $\sigma_p = +1$, and states in the Dirac sea $|\alpha\rangle$ (antiparticle states) with negative energies. Because of the no-sea approximation, the orbits with negative energies $|\alpha\rangle$ are left unoccupied; therefore we have $\sigma_\alpha = +1$. However, as shown in Ref. [44], the numerical contribution of the diagrams with intermediate states α with negative energy is very small because of the large energy denominators in the corresponding terms of the self-energy (18). The index μ in Eq. (18) labels the various phonons taken into account. Ω^μ is their frequency, ρ^μ is their transition density, and the phonon vertices γ^μ_{kl} determine their coupling to the nucleons:

$$\gamma^\mu_{kl} = \sum_{k'l'} \tilde{V}_{kl', lk'} \rho^\mu_{k'l'}. \quad (19)$$

$$\Sigma^e_{p'p''} = \quad + \quad + \quad$$
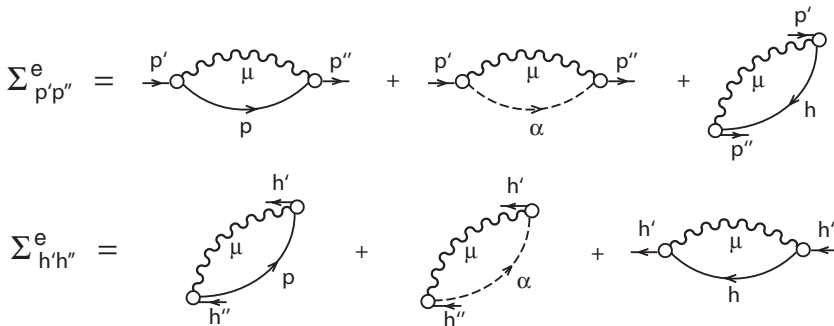
$$\Sigma^e_{h'h''} = \quad + \quad + \quad$$

FIG. 1. Particle $\Sigma^e_{p'p''}$ and hole $\Sigma^e_{h'h''}$ components of the relativistic mass operator in the graphical representation. Solid and dashed lines with arrows denote one-body propagators for particle (p), hole (h), and antiparticle (α) states. Wavy lines denote phonon (μ) propagators, empty circles are the particle-phonon coupling amplitudes γ^μ.

$\tilde{V}_{kl',lk'}$ denotes the relativistic matrix element of the residual interaction. It is obtained as a functional derivative of the relativistic mean field with respect to relativistic density matrix ρ, that is,

$$\tilde{V}_{kl',lk'} = \frac{\delta \tilde{\Sigma}_{l'k'}}{\delta \rho_{lk}}. \tag{20}$$

We use the linearized version of the model, which assumes that ρ^{μ} is not influenced by the particle-phonon coupling and can be computed within the relativistic RPA approximation. As long as we neglect the nonlinear self-couplings of the mesons or the density dependence of the coupling constants g_m in Eq. (3), the matrix elements $\tilde{V}_{kl',lk'}$ in Eq. (19) have a simple Yukawa form. However, such effects have to be taken into account to guarantee full self-consistency of the RRPA equations, and we find more complicated expressions, which are discussed in detail in Appendix A. In the applications investigated in Sec. III, we use the nonlinear parameter set NL3 [45] for the solution of the static Dirac equation (11) as well as for the calculation of the matrix elements (20).

C. Response function

Nuclear dynamics of an even-even nucleus in a weak external field is described by the linear response function $R(14, 23)$ which is the solution of the Bethe-Salpeter equation (BSE) in the p-h channel. In the beginning, it is convenient to consider this equation in the time representation. Let us include the time variable into the single-particle indices, setting $1 = \{k_1, t_1\}$. In this notation, the BSE for the response function R reads

$$R(14, 23) = G(1, 3)G(4, 2) - i \sum_{5678} G(1, 5)G(6, 2)$$
$$\times V(58, 67)R(74, 83), \tag{21}$$

where the summation over the number indices $1, 2, \ldots$ implies integration over the respective time variables. The function G is the exact single-particle Green's function, and V is the amplitude of the effective interaction irreducible in the p-h channel. This amplitude is determined as a variational derivative of the full self-energy Σ with respect to the exact single-particle Green's function, i.e.,

$$V(14, 23) = i \frac{\delta \Sigma(4, 3)}{\delta G(2, 1)}. \tag{22}$$

Introducing the free response $R^0(14, 23) = G(1, 3)G(4, 2)$, the BSE (21) can be written in a shorthand notation as

$$R = R^0 - i R^0 V R. \tag{23}$$

For the sake of simplicity, we will use this shorthand notation frequently in the following discussions. Since the self-energy in Eq. (7) has two parts, $\Sigma = \tilde{\Sigma} + \Sigma^e$, the effective interaction V in Eq. (21) is a sum of the static RMF interaction $\tilde{V}$ and time-dependent terms V^e,

$$V = \tilde{V} + V^e, \tag{24}$$

where (with $t_{12} = t_1 - t_2$)

$$\tilde{V}(14, 23) = \tilde{V}_{k_1k_4, k_2k_3}\delta(t_{31})\delta(t_{21})\delta(t_{34}) \tag{25}$$

is the static part of the interaction [see Eq. (20)], and

$$V^e(14, 23) = i \frac{\delta \Sigma^e(4, 3)}{\delta G(2, 1)} \tag{26}$$

contains the energy dependence. In the space of the Dirac basis (11), the amplitude V^e has the form

$$V^e_{kl',lk'}(\omega, \varepsilon, \varepsilon') = \sum_{\mu,\sigma} \frac{\sigma \gamma^{\mu(\sigma)*}_{k'k} \gamma^{\mu(\sigma)}_{l'l}}{\varepsilon - \varepsilon' + \sigma(\Omega^{\mu} - i\eta)}. \tag{27}$$

To make the BSE (21) more convenient for the subsequent analysis, we eliminate the exact Green's function G and rewrite it in terms of the mean-field Green's function $\tilde{G}$ determined as

$$\tilde{G}(1, 2) = -i\sigma_{k_1}\delta_{k_1k_2}\theta(\sigma_{k_1}\tau)e^{-i\varepsilon_{k_1}\tau}, \quad \tau = t_1 - t_2, \tag{28}$$

where $\theta(t)$ is the Heaviside function. After a Fourier transformation in time, this reads

$$\tilde{G}_{k_1k_2}(\varepsilon) = \frac{\delta_{k_1k_2}}{\varepsilon - \varepsilon_{k_1} + i\sigma_{k_1}\eta}. \tag{29}$$

Using the connection between $\tilde{G}$ and G in the Nambu form

$$\tilde{G}^{-1}(1, 2) = G^{-1}(1, 2) + \Sigma^e(1, 2), \tag{30}$$

one can rewrite Eq. (21) as

$$R = \tilde{R}^0 - i\tilde{R}^0 W R, \tag{31}$$

with $\tilde{R}^0(14, 23) = \tilde{G}(1, 3)\tilde{G}(4, 2)$, and W is a new interaction of the form

$$W = \tilde{V} + W^e, \tag{32}$$

where

$$W^e(14, 23) = V^e(14, 23) + i\Sigma^e(1, 3)\tilde{G}^{-1}(4, 2)$$
$$+ i\tilde{G}^{-1}(1, 3)\Sigma^e(4, 2) - i\Sigma^e(1, 3)\Sigma^e(4, 2). \tag{33}$$

Since the mean-field Green's function $\tilde{G}$ in Eq. (29) is known, one has a more convenient starting point for the solution of the Bethe-Salpeter equation (31) than with the unknown exact single-particle Green's function, but the effective interaction W in Eq. (32) becomes more complicated. The graphical representation of Eq. (31) is shown in Fig. 2.

In addition to the static interaction $\tilde{V}$, the effective interaction W contains diagrams with energy-dependent self-energies and an energy-dependent *induced interaction*, where a phonon is exchanged between the particle and the hole. Hereafter we omit the term $i\Sigma^e(3, 1)\Sigma^e(2, 4)$ in Eq. (33) for the following reasons. This term compensates the multiple counting of the particle-phonon coupling arising from the two previous terms in Eq. (33). However, this multiple counting does not take place within the time blocking approximation (see below) if the backward-going propagators are not taken
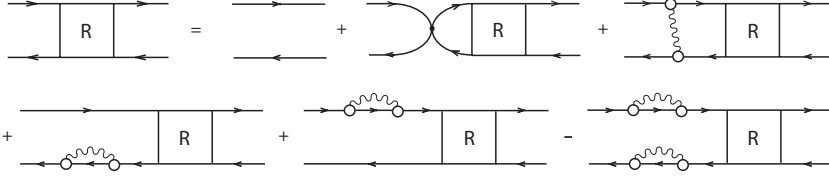
into account. Components containing the backward-going propagators within 1p1h⊗phonon configurations require a special consideration. They have been analyzed in great detail in Refs. [34–36]. In the present work, they are fully neglected, and therefore the term $i\Sigma^e(3, 1)\Sigma^e(2, 4)$ has also to be omitted. However, we have to emphasize that we only neglect ground state correlations (backward-going diagrams) caused by the particle-phonon coupling. All the RPA ground state correlations are taken into account, because it is well known that they play a central role for the conservation of currents and sum rules. We consider that this is a reasonable approximation, which has been applied and discussed in many nonrelativistic models (see, e.g., Refs. [29–38] and references therein).

Considering a Fourier transformation of the BSE (31) in time

$$
\begin{aligned}
R_{k_1 k_4, k_2 k_3}&(\omega, \varepsilon) \\
&= \tilde{G}_{k_1 k_3}(\varepsilon + \omega)\tilde{G}_{k_4 k_2}(\varepsilon) + \sum_{k_5 k_6 k_7 k_8} \tilde{G}_{k_1 k_5}(\varepsilon + \omega)\tilde{G}_{k_6 k_2}(\varepsilon) \\
&\quad \times \int_{-\infty}^{\infty} \frac{d\varepsilon'}{2\pi i} W_{k_5 k_8, k_6 k_7}(\omega, \varepsilon, \varepsilon')R_{k_7 k_4, k_8 k_3}(\omega, \varepsilon'),
\end{aligned}
\tag{34}
$$

one finds that both the solution of this equation R and its kernel W are singular with respect to the energy variables. Another difficulty arises because Eq. (31) contains integrations over all time points of the intermediate states. This means that many configurations which are actually more complex than 1p1h⊗phonon are contained in the exact response function. In Ref. [34], a special time-projection technique was introduced to block the p-h propagation through these complex intermediate states. It has been shown that for this type of response it is possible to reduce the integral equation (34) to a relatively simple algebraic equation. Obviously, this method can be applied straightforwardly in our case, too.

Starting from the Bethe-Salpeter equation (31), we divide the problem of finding the exact response function into two parts. First, we calculate the *correlated propagator* R^e, which describes the propagation under the influence of the interaction W^e,

$$
R^e = \tilde{R}^0 - i\tilde{R}^0 W^e R^e.
\tag{35}
$$

It contains all the effects of particle-phonon coupling and all the singularities of the integral part of the initial BSE. Second, we solve the remaining equation for the full response function R

$$
R = R^e - iR^e\tilde{V}R.
\tag{36}
$$

Equation (36) contains only the static effective interaction $\tilde{V}$ and can be easily solved if R^e is known. Thus, the main problem is to calculate the correlated propagator R^e.

D. Time blocking approximation and subtraction method

To calculate the correlated propagator R^e, we represent this quantity as an infinite series of graphs which contain mean-field p-h propagators alternated with single interaction acts. This can be expressed by the system of equations

$$
R^e = \tilde{R}^0 - i\tilde{R}^0\Gamma^e\tilde{R}^0,
\tag{37}
$$

$$
\Gamma^e = W^e - iW^e\tilde{R}^0\Gamma^e.
\tag{38}
$$

According to the main idea of the time blocking approximation (TBA), we modify the integral part of Eq. (38) making use of the time-projection operator in the form [34]

$$
\Theta(14, 23) = \delta_{\sigma_{k_1}, -\sigma_{k_2}}\delta_{k_1 k_3}\delta_{k_2 k_4}\theta(\sigma_{k_1}t_{14})\theta(\sigma_{k_1}t_{23}),
\tag{39}
$$

where $\theta(t)$ is the Heaviside function. This projection operator is introduced into the mean-field propagator $\tilde{R}^0$ in the integral part of Eq. (38) to order the p-h propagation in time and thus to separate in time the acts of the particle-phonon interaction from each other and to exclude configurations which are more complex than 1p1h⊗phonon. We replace in Eq. (38) the mean-field propagator $\tilde{R}^0$ by

$$
\tilde{R}^0(14, 23) \rightarrow \tilde{R}^0(14, 23)\Theta(14, 23)
\tag{40}
$$

and obtain instead of Eq. (38)

$$
\begin{aligned}
\Gamma^e(14, 23) &= W^e(14, 23) + \frac{1}{i}\sum_{5678}W^e(16, 25)\tilde{R}^0(58, 67) \\
&\quad \times \Theta(58, 67)\Gamma^e(74, 83).
\end{aligned}
\tag{41}
$$

After a Fourier transformation in time, we restrict ourselves to the response function $R_{k_1 k_4, k_2 k_3}(\omega)$

$$
\begin{aligned}
R_{k_1 k_4, k_2 k_3}(\omega) &= -i\int_{-\infty}^{\infty} dt_1\dot{d}t_2 dt_3 dt_4 \delta(t_1 - t_2)\delta(t_3 - t_4) \\
&\quad \times \delta(t_4)e^{i\omega t_{13}}R(14, 23),
\end{aligned}
\tag{42}
$$

which depends only on one energy variable ω.

The time projection by the operator (39) leads to a separation of integrations in Eq. (34), and we find an algebraic equation for the function (42),

$$
\begin{aligned}
R_{k_1 k_4, k_2 k_3}(\omega) &= \tilde{R}^0_{k_1 k_4, k_2 k_3}(\omega) + \sum_{k_5 k_6 k_7 k_8} \tilde{R}^0_{k_1 k_6, k_2 k_5}(\omega) \\
&\quad \times \bar{W}_{k_5 k_8, k_6 k_7}(\omega)R_{k_7 k_4, k_8 k_3}(\omega),
\end{aligned}
\tag{43}
$$

or in shorthand notation,

$$
R(\omega) = \tilde{R}^0(\omega) + \tilde{R}^0(\omega)\bar{W}(\omega)R(\omega),
\tag{44}
$$

where

$$\bar{W}_{k_1 k_4, k_2 k_3}(\omega) = \tilde{V}_{k_1 k_4, k_2 k_3} + \Phi_{k_1 k_4, k_2 k_3}(\omega), \qquad (45)$$

and

$$\tilde{R}^0_{k_1 k_4, k_2 k_3}(\omega) = \tilde{R}_{k_1 k_2}(\omega)\delta_{k_1 k_3}\delta_{k_2 k_4}. \qquad (46)$$

$\tilde{R}_{k_1 k_2}(\omega)$ is the mean-field propagator

$$\tilde{R}_{ph}(\omega) = -\frac{1}{\varepsilon_{ph} - \omega}, \quad \tilde{R}_{\alpha h}(\omega) = -\frac{1}{\varepsilon_{\alpha h} - \omega}, \qquad (47)$$

$$\tilde{R}_{hp}(\omega) = -\frac{1}{\varepsilon_{ph} + \omega}, \quad \tilde{R}_{h\alpha}(\omega) = -\frac{1}{\varepsilon_{\alpha h} + \omega}, \qquad (48)$$

$\varepsilon_{ph} = \varepsilon_p - \varepsilon_h$ and Φ is the particle-phonon coupling amplitude with the components

$$\Phi_{ph', hp'}(\omega) = \sum_\mu \left[\delta_{pp'} \sum_{h''} \frac{\gamma^\mu_{h''h} \gamma^{\mu*}_{h''h'}}{\omega - \varepsilon_p + \varepsilon_{h''} - \Omega^\mu} \right.$$
$$+ \delta_{hh'} \left(\sum_{p''} \frac{\gamma^\mu_{pp''} \gamma^{\mu*}_{p'p''}}{\omega - \varepsilon_{p''} + \varepsilon_h - \Omega^\mu} \right.$$
$$\left. + \sum_{\alpha''} \frac{\gamma^\mu_{p\alpha''} \gamma^{\mu*}_{p'\alpha''}}{\omega - \varepsilon_{\alpha''} + \varepsilon_h - \Omega^\mu} \right)$$
$$- \left(\frac{\gamma^\mu_{pp'} \gamma^{\mu*}_{hh'}}{\omega - \varepsilon_{p'} + \varepsilon_h - \Omega^\mu} \right.$$
$$\left. \left. + \frac{\gamma^{\mu*}_{p'p} \gamma^\mu_{h'h}}{\omega - \varepsilon_p + \varepsilon_{h'} - \Omega^\mu} \right) \right], \qquad (49)$$

$$\Phi_{\alpha h', h\alpha'}(\omega) = \sum_\mu \left[\delta_{\alpha\alpha'} \sum_{h''} \frac{\gamma^\mu_{h''h} \gamma^{\mu*}_{h''h'}}{\omega - \varepsilon_\alpha + \varepsilon_{h''} - \Omega^\mu} \right.$$
$$+ \delta_{hh'} \left(\sum_{\alpha''} \frac{\gamma^\mu_{\alpha\alpha''} \gamma^{\mu*}_{\alpha'\alpha''}}{\omega - \varepsilon_{\alpha''} + \varepsilon_h - \Omega^\mu} \right.$$
$$\left. + \sum_{p''} \frac{\gamma^\mu_{\alpha p''} \gamma^{\mu*}_{\alpha'p''}}{\omega - \varepsilon_{p''} + \varepsilon_h - \Omega^\mu} \right)$$
$$- \left(\frac{\gamma^\mu_{\alpha\alpha'} \gamma^{\mu*}_{hh'}}{\omega - \varepsilon_{\alpha'} + \varepsilon_h - \Omega^\mu} \right.$$
$$\left. \left. + \frac{\gamma^{\mu*}_{\alpha'\alpha} \gamma^\mu_{h'h}}{\omega - \varepsilon_\alpha + \varepsilon_{h'} - \Omega^\mu} \right) \right]. \qquad (50)$$

Indices $p, \alpha,$ and h traditionally denote the particle, antiparticle, and hole types of the Dirac states, respectively. There are, in principle, also nonzero amplitudes of the types $\Phi_{ph', h\alpha}, \Phi_{\alpha h', hp}$ which cause transitions of particle-hole (p-h) to antiparticle-hole (α-h) pairs. However, we neglect them in the present work because, as investigated in Ref. [44], the effect of these kinds of terms on self-energy is very small, whereas they require a lot of numerical effort. The reason is that these components as well as the component (50) contain large energy denominators. As already mentioned, amplitudes of the types $\Phi_{pp', hh'}$ and $\Phi_{hh', pp'}$ are also disregarded within our

approximation. Therefore, ground state correlations are taken into account only on the RPA level, because of the presence of the $\tilde{V}_{pp', hh'}, \tilde{V}_{hh', pp'}$ terms of the static interaction in Eq. (43). By definition, the propagator $R(\omega)$ in Eq. (43) contains only configurations which are not more complex than 1p1h $\otimes$ phonon.

An important correction has to be made in Eq. (43). Having been adjusted to experimental data, the RMF ground state effectively contains many correlations and, in particular, admixtures of phonons. Therefore in our approach, as well as in other approaches beyond RPA where more complex configurations are taken into account explicitly, these admixtures would lead to double counting of correlations. In the present method, all the correlations entering through the admixture of phonons are taken care of by an additional interaction term: $\Phi(\omega)$. Part of this interaction is therefore already contained in the static mean-field interaction $\tilde{V}$. Since the parameter of the density functional and, as a consequence, the effective interaction $\tilde{V}$ are adjusted to experimental ground state properties at the energy $\omega = 0$, this part of the interaction $\Phi(\omega)$, which is already contained in $\tilde{V}$ is given by $\Phi(0)$. To avoid double counting of correlations, a subtraction procedure was developed in Ref. [37] that removes this part. As a consequence, one has to replace the additional interaction Φ in Eq. (45) by the function $\delta\Phi$, that is,

$$\Phi(\omega) \rightarrow \delta\Phi(\omega) = \Phi(\omega) - \Phi(0). \qquad (51)$$

The physical meaning of this subtraction is clear: the average value of the particle-vibration coupling amplitude Φ at the ground state is supposed to be contained already in the residual interaction $\tilde{V}$, therefore we should take into account only the additional energy dependence, i.e., $\delta\Phi(\omega) = \Phi(\omega) - \Phi(0)$ on top of the effective interaction $\tilde{V}$. Instead of Eq. (43), we finally solve the following response equation

$$R = \tilde{R}^0 + \tilde{R}^0[\tilde{V} + \delta\Phi]R. \qquad (52)$$

E. Strength function and transition densities

To describe the observed spectrum of the excited nucleus in a weak external field P, as for instance a dipole field, one needs to calculate the strength function

$$S(E) = -\frac{1}{\pi} \lim_{\Delta \to +0} \mathrm{Im}\Pi_{pp}(E + i\Delta), \qquad (53)$$

expressed through the polarizability Π_{pp} defined as

$$\Pi_{pp}(\omega) = P^\dagger R(\omega) P$$
$$:= \sum_{k_1 k_2 k_3 k_4} P^*_{k_1 k_2} R_{k_1 k_4, k_2 k_3}(\omega) P_{k_3 k_4}. \qquad (54)$$

The imaginary part Δ of the energy variable is introduced for convenience in order to obtain a more smoothed envelope of the spectrum. This parameter has the meaning of an additional artificial width for each excitation. This width effectively emulates contributions from configurations not taken into account explicitly in our approach.

To calculate the strength function, it is convenient to convolute Eq. (52) with an external field operator and introduce the density matrix variation $\delta\rho$ in the external field P:

$$\delta\rho_{k_1 k_2}(\omega) = \sum_{k_3 k_4} R_{k_1 k_4, k_2 k_3}(\omega) P_{k_3 k_4}, \qquad (55)$$

$$\delta\rho^0_{k_1 k_2}(\omega) = \sum_{k_3 k_4} \tilde{R}^0_{k_1 k_4, k_2 k_3}(\omega) P_{k_3 k_4}. \qquad (56)$$

Using Eq. (52), we find that $\delta\rho(\omega)$ obeys the equation

$$\delta\rho(\omega) = \delta\rho^0(\omega) + \tilde{R}^0(\omega)(\tilde{V} + \delta\Phi(\omega))\delta\rho(\omega), \qquad (57)$$

and the strength function is expressed as

$$S(E) = -\frac{1}{\pi} \lim_{\Delta \to +0} \text{Im} \text{Tr}[P^\dagger \delta\rho(E + i\Delta)]. \qquad (58)$$

The BSE (52) gives us also the possibility of calculating the transition density

$$\rho^\nu_{k_1 k_2} = \langle 0|\psi^\dagger_{k_2}\psi_{k_1}|\nu\rangle \qquad (59)$$

for the excited state $|\nu\rangle$ at the energy Ω^ν. In the vicinity of Ω^ν the response function has a simple pole structure

$$R^\nu_{k_1 k_4, k_2 k_3}(\omega) \approx \frac{\rho^\nu_{k_1 k_2}\rho^{\nu *}_{k_3 k_4}}{\omega - \Omega^\nu}, \qquad (60)$$

which leads to

$$\rho^\nu_{k_1 k_2} = \lim_{\Delta \to +0}\sqrt{\frac{\Delta}{\pi S(\Omega^\nu)}}\, \text{Im}\,\delta\rho_{k_1 k_2}(\Omega^\nu + i\Delta). \qquad (61)$$

To determine the norm of the transition densities, it is convenient to rewrite Eq. (52) in the form

$$((\tilde{R}^0)^{-1}(\omega) - \tilde{V} - \delta\Phi(\omega))R(\omega) = 1. \qquad (62)$$

Using Eq. (60) and taking the derivative with respect to ω, we obtain the generalized normalization condition

$$\rho^{\nu *}\left[N - \frac{d\Phi}{d\omega}\bigg|_{\omega=\Omega^\nu}\right]\rho^\nu = 1, \qquad (63)$$

with the RPA norm

$$N_{k_1 k_4, k_2 k_3} = \sigma_{k_1}\delta_{\sigma_{k_1}, -\sigma_{k_2}}\delta_{k_1 k_3}\delta_{k_2 k_4}.$$

In the limiting case of an energy-independent interaction, i.e., if one neglects $\Phi(\omega)$, this reduces to the usual RPA normalization

$$\sum_{ph}\left(|\rho^\nu_{ph}|^2 - |\rho^\nu_{hp}|^2\right) = 1. \qquad (64)$$

In the particle-vibration coupling model, the quantity $N\frac{d}{d\omega}\Phi$ in Eq. (63) is a nonpositively definite matrix. Therefore, all the eigenvalues of the operator $[1 - N(\frac{d}{d\omega}\Phi)\,|_{\omega=\Omega^\nu}\,]^{-1}$ are less than or equal to unity, in analogy to the spectroscopic factor of a single-particle state. For this reason, the sum

$$\sum_{ph}\left(|\rho^\nu_{ph}|^2 - |\rho^\nu_{hp}|^2\right) \qquad (65)$$

is practically always less than unity. The reduction of the norm is caused by the spreading of the strength over 1p1h $\otimes$ phonon configurations.

III. NUMERICAL DETAILS, RESULTS, AND DISCUSSION

A. General scheme of the calculations

The method developed in the last section is applied to a quantitative description of isoscalar monopole and isovector dipole giant resonances in the even-even spherical nuclei ^{208}Pb and ^{132}Sn. Our calculations are based on the energy functional with the nonlinear parameter set NL3 [45]. The scheme consists of three main parts:

(i) The Dirac equation for single nucleons together with the Klein-Gordon equations for meson fields are solved simultaneously in a self-consistent way to obtain the single-particle basis (Dirac basis).

(ii) The RRPA equations [16] are solved with the static interaction $\tilde{V}$ of Eq. (20) to determine the low-lying collective vibrations (phonons). These two sets of particles (holes) and phonons form the multitude of 1p1h$\otimes$phonon configurations which enter the particle-phonon coupling amplitude $\delta\Phi(\omega)$.

(iii) Eq. (57) for the density matrix variation $\delta\rho$ in the external field P is solved using this additional amplitude in the effective interaction $\tilde{V} + \delta\Phi(\omega)$. Equation (58) finally allows us to calculate the strength function corresponding to the operator P. It is found that the energy-dependent term $\delta\Phi(\omega)$, which describes the change of the effective interaction due to the energy dependence of the particle-vibration coupling, provides a considerable enrichment of the calculated spectrum compared to the spectrum obtained by the pure RRPA.

B. Choice of representation and basic approximations

Equation (57) for $\delta\rho$ can be solved in various representations. In Dirac space, its dimension is the number of p-h pairs. In relativistic nuclear calculations, it is often important to take into account the contributions of the Dirac sea, and then the total number of p-h and α-h pairs entering Eq. (57) increases considerably with the nuclear mass number because of the high level density. As investigated in a series of RRPA calculations [16,48], the completeness of the p-h (α-h) basis is very important for calculations of giant resonance characteristics as well as for current conservation and a proper treatment of symmetries, in particular, the dipole spurious state originating from the violation of translation symmetry on the mean-field level. On the other hand, the use of a large basis requires considerable numerical effort, and therefore it is reasonable to solve Eq. (57) in a different, more appropriate representation.

Two facts simplify our practical calculations:

(i) Because of the pole structure of the $\delta\Phi$ amplitude, the effects of particle-phonon coupling are only important in the vicinity of the Fermi surface; therefore one can

restrict the number of p-h configurations in this case much more than in the case of the static interaction $\tilde{V}$.

(ii) The effective interaction $\tilde{V}$, which is based on the exchange of mesons, contains only direct terms and no exchange terms. Therefore, it can be written as a sum of separable interactions.

To exploit these two effects, we solve the response equation for a fixed value of the energy ω in two steps. First, we calculate the *correlated propagator* $R^e(\omega)$, which describes the propagation under the influence of the interaction $\delta\Phi(\omega)$,

$$R^e = \tilde{R}^0 + \tilde{R}^0 \delta\Phi R^e. \quad (66)$$

It contains all the effects of particle-phonon coupling and all the singularities of the integral part of the initial BSE. Since $\delta\Phi$ is not separable, Eq. (66) has to be solved in Dirac space. This requires in principle for each value of ω the inversion of a very large matrix. However, the numerical effort can be reduced considerably by taking into account that the effects of the particle-phonon coupling are only important in the vicinity of the Fermi surface. Therefore, the summation in Eq. (66) is performed only among the p-h pairs with $\varepsilon_{ph} \leqslant \varepsilon_{\text{win}}$. Consequently, the correlated propagator R^e differs from the mean-field propagator $\tilde{R}^0$ only within this window. This approximation has been investigated numerically by explicit calculations with different window sizes, as discussed below. In contrast to Eq. (52), this equation contains only the static effective interaction and it is solved in the large basis of p-h and α-h configurations.

In the second step, we solve the remaining equation for the full response function $R(\omega)$:

$$R = R^e + R^e \tilde{V} R. \quad (67)$$

In contrast to Eq. (52), this equation contains only the static effective interaction.

Now we exploit the fact that the one-boson exchange (OBE) interaction discussed in Appendix C is separable in momentum space. It can be expressed as

$$\tilde{V}_{k_1 k_4, k_2 k_3} = \sum_c d_c Q^{(c)}_{k_1 k_2} Q^{(c)*}_{k_3 k_4}, \quad (68)$$

where the channel index $c = (q, m)$ is given by the momentum q transferred in the exchange process of the corresponding meson labeled by the index m. The parameters d_c are given by the meson propagators. We now can use the well-known techniques of the response formalism with separable interactions (see, for instance, Ref. [49]). We define

$$R_{cc'}(\omega) = \sum_{k_1 k_2 k_3 k_4} Q^{(c)*}_{k_1 k_2} R_{k_1 k_4, k_2 k_3}(\omega) Q^{(c')}_{k_3 k_4} \quad (69)$$

and find from Eq. (67)

$$R_{cc'} = R^e_{cc'} + \sum_{c''} R^e_{cc''} d_{c''} R_{c''c'} = R^e_{cc'} + (R^e dR)_{cc'}. \quad (70)$$

This equation can be solved by matrix inversion

$$R = (1 - R^e d)^{-1} R^e. \quad (71)$$

Finally, we transform Eq. (57) to the momentum space, which is equivalent to using the external field as an additional channel $c = p$, and obtain from Eq. (69) the full response

$$\delta\rho_c = \delta\rho^e_c + \sum_{c'} R^e_{cc'} d_{c'} \delta\rho_{c'}, \quad (72)$$

and the polarizability (54)

$$\begin{aligned} \Pi_{pp} &= P^\dagger R P = P^\dagger R^e P + \sum_c \delta\rho^{e*}_c d_c \delta\rho_c \\ &= R^e_{pp} + \sum_{cc'} \delta\rho^{e*}_c d_c (1 - R^e d)^{-1}_{cc'} \delta\rho^e_{c'}. \end{aligned} \quad (73)$$

The rank of vectors and matrices entering Eq. (72) is determined by the number of mesh points in q space and the number of meson channels. In particular, it does not depend on the mass number of the nucleus. In realistic calculations, the rank of Eq. (71) in the momentum space is around 500, and obviously the numerical effort does not depend considerably on the total dimension of p-h and α-h subspaces. However, if one stays in the Dirac basis, the latter dimension is exactly the rank of arrays in Eq. (43). One should bear in mind that in practice, both subspaces (p-h and α-h) are truncated at some energy differences ε_{ph} and $\varepsilon_{\alpha h}$ which are large enough so that a further increase of these values does not influence the results. In light nuclei with relatively small level density, the total dimension of p-h and α-h subspaces is comparable and could be even smaller than the rank of Eq. (72); therefore, working in the Dirac basis is more preferable. For heavy nuclei, the dimension of the Dirac basis becomes huge; therefore, using the momentum space is more justified.

C. Numerical details

To ensure numerical correctness of our codes, we solved the response equation for $\delta\rho$ in both momentum space [Eq. (72)] and Dirac space [Eq. (57)] and obtained identical results. Both Fermi and Dirac subspaces were truncated at energies far from the Fermi surface. In the present work as well as in Ref. [44], we fix the limits $\varepsilon_{ph} < 100$ MeV and $\varepsilon_{\alpha h} > -1800$ MeV with respect to the positive continuum. A small artificial width of 200 keV was introduced as an imaginary part of the energy variable ω to have a smooth envelope of the calculated curves. The energies and amplitudes of the most collective phonon modes with spin and parity 2^+, 3^-, 4^+, 5^-, and 6^+ were calculated with the same restrictions and selected using the same criterion as in the Ref. [44] and in many other nonrelativistic investigations in this context. Only phonons with energies below the neutron separation energy enter the phonon space, since the contributions of the higher lying modes are found to be small. Test calculations in the framework of the approach [37,38] without the restriction of the phonon space by the energy resulted in a small deviation of the strength function as well as a change of the mean energies and widths of the resonances comparable with the smearing parameter (imaginary part of the energy variable) used in the calculations. This is the natural result, because the

physical sense of this parameter is to emulate contributions of the configurations which are not taken into account explicitly.

Because of the pole structure of the particle-phonon coupling amplitude [Eqs. (49) and (50)], its contributions to the final result decrease considerably when we go away from the Fermi surface. Therefore, this coupling has been taken into account only within the p-h energy window $\varepsilon_{ph} \leqslant 30$ MeV around the Fermi surface. It has been checked that further increase of this window does not influence significantly the results.

It is important to note that although a large number of configurations of the 1p1h⊗phonon type are taken into account explicitly in our approach, nevertheless we stay in the same p-h (α-h) space as in the RRPA; therefore, the problem of completeness of the phonon basis does not arise, and so the phonon subspace can be truncated in the above-mentioned way. Another essential point is that on all three stages of our calculations, the same relativistic nucleon-nucleon interaction $\tilde{V}$ [Eq. (20)] has been employed. The vertices $\gamma_{k_1 k_2}^{\mu}$ [Eq. (19)] entering the term $\delta\Phi(\omega)$ are calculated with the same force. Therefore, no further parameters are needed. Our calculational scheme is fully consistent.

The subtraction procedure (51) developed in Ref. [37] for the self-consistent scheme has been incorporated in our approach. As mentioned above, this procedure removes the static contribution of the particle-phonon coupling from the p-h interaction. It takes into account only the additional energy dependence introduced by the dynamics of the system. It has been found in the present calculations as well as in the calculations of Ref. [38] that within the relatively large energy interval (0–30 MeV), the subtraction procedure provides a noticeable increase of the mean energy of the giant dipole resonance (0.8 MeV for the lead region) and gives rise to the change by a few percents in the sum rule. This procedure restores the response at zero energy, and therefore it does not disturb the symmetry properties of the RRPA calculations. The zero energy modes connected with the spontaneous symmetry breaking in the mean-field solutions, as for instance the translational mode in the dipole case, remain at exactly the same position after the inclusion of the particle-vibration coupling. In practice, however, because of the limited number of oscillator shells in our calculations, this state is found already in RRPA without particle-vibration coupling at a few hundreds keV above zero. In cases where the results depend strongly on a proper separation of this spurious state, as for instance for investigations of the pygmy dipole resonance in neutron rich systems, we have to include a large number of p-h configurations in the RRPA solution.

D. Isoscalar monopole and isovector dipole resonances in ²⁰⁸Pb and ¹³²Sn

The calculated strength functions for the isoscalar monopole resonance in ²⁰⁸Pb and ¹³²Sn are shown in Fig. 3. The fragmentation of the resonance caused by the particle-phonon coupling is clearly demonstrated, although the spreading width of the monopole resonance is not large because of a strong cancellation between the self-energy diagrams and
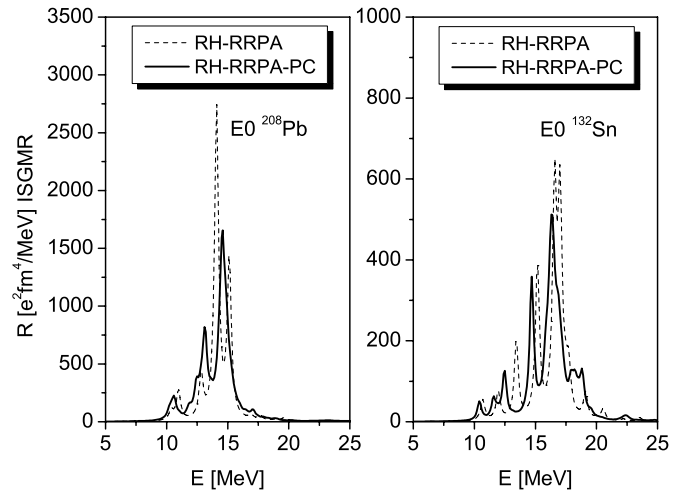

FIG. 3. Isoscalar monopole resonance in ²⁰⁸Pb and ¹³²Sn obtained within two approaches: RRPA (dashed line) and RRPA with particle-phonon coupling RRPA-PC (solid line). Both computations were performed with relativistic Hartree (RH) mean field and employ NL3 parameter set for RMF forces.

diagrams with the phonon exchange (see Fig. 2). This fact has also been discussed in detail in Refs. [29,30], and it is not disturbed by the subtraction procedure (51) because this cancellation takes place in $\Phi(0)$ as well as in $\Phi(\omega)$.

To compare the spreading of the theoretical strength distributions with experimental data, we deduce mean energies $\langle E \rangle$ and width parameters Γ by fitting our theoretical strength distribution in a certain energy interval to a Lorentz curve in the same way as done in the experimental investigations. The mean energies and width parameters obtained in this way are shown in the Table I. We display as experimental data the numbers adopted in Ref. [50] from the evaluation of a series of data obtained in different experiments for the isoscalar monopole resonance in ²⁰⁸Pb.

The calculated photoabsorption cross sections

$$\sigma_{E1}(E) = \frac{16\pi^3 e^2}{9\hbar c} E S_{E1}(E) \qquad (74)$$

for the isovector dipole resonance in ²⁰⁸Pb and ¹³²Sn are given in the Figs. 4 and 5, respectively. The left panels show

TABLE I. Lorentz fit parameters of isoscalar $E0$ strength function in ²⁰⁸Pb and ¹³²Sn calculated within RRPA and RRPA extended by the particle-phonon coupling model (RRPA-PC) as compared with experimental data. The fit was carried out in the interval from B_n to roughly 20 MeV.

		$\langle E \rangle$ (MeV)	Γ (MeV)
²⁰⁸Pb	RRPA	14.16	1.71
	RRPA-PC	14.05	2.36
	Exp. [50]	13.73(20)	2.58(20)
¹³²Sn	RRPA	16.10	2.63
	RRPA-PC	16.01	3.09
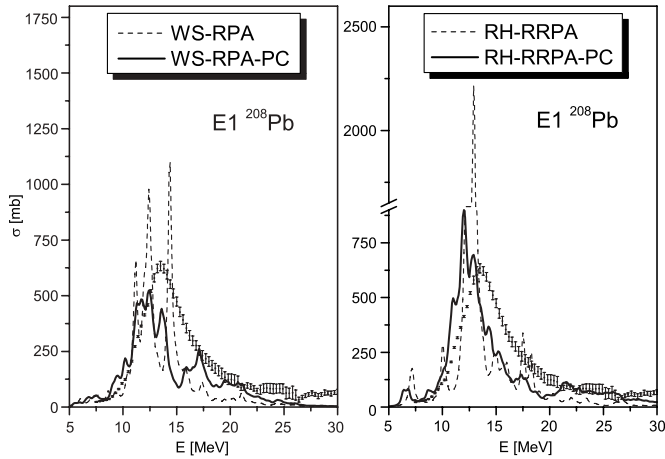
FIG. 4. Isovector $E1$ resonance in ^{208}Pb. Details are given in the text.

FIG. 5. Same as Fig. 4, but for ^{132}Sn.

the results obtained within the nonrelativistic approach with Woods-Saxon (WS) single-particle input and Landau-Migdal (LM) forces described in Ref. [38]. They are compared in the right panel with the relativistic fully consistent theory developed in the present work. The underlying Lagrangian has the parameter set NL3 [45]. In Fig. 4, we have displayed experimental data with error bars taken from Ref. [51]. To make the comparison reasonable, calculations within the nonrelativistic framework were performed with box boundary conditions for the Schrödinger equation in r space, which ensures completeness of the single-particle basis.

The corresponding Lorentz fit parameters in the two energy intervals B_n–25 and 0–30 MeV (B_n is the neutron separation energy) are included in Table II and compared with the data of Refs. [51,52]. We notice that the inclusion of particle-phonon coupling in the RRPA calculation induces a pronounced fragmentation of the photoabsorption cross sections and brings the width of the GDR in much better agreement with the data, both for ^{208}Pb and ^{132}Sn.

The fragmentation of the resonance introduced by the particle-phonon coupling is clearly demonstrated in both cases. Also, one finds more or less the same level of agreement between theory and experimental data for these two calculations. In the case of the isovector $E1$ resonance in ^{132}Sn, however, this is not so clear, because the cross section and the integral
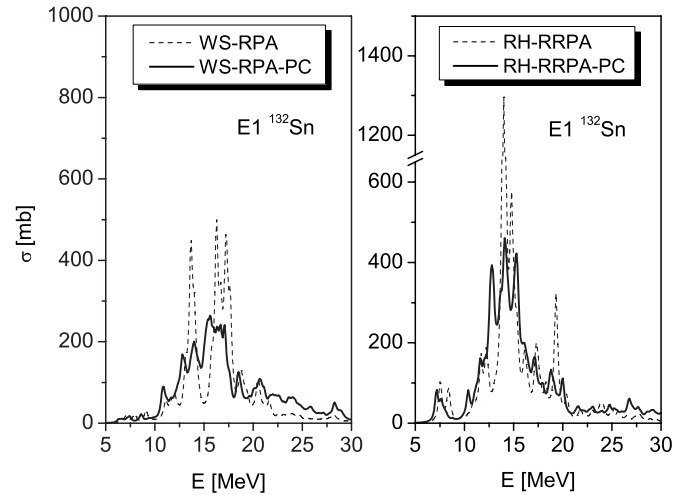
characteristics of the resonance obtained in the experiment of Ref. [52] are given with relatively large error bars. In ^{208}Pb, our self-consistent relativistic approach reproduces the shape of the giant dipole resonance much better than the nonrelativistic one, although the whole resonance is shifted by about 0.5 MeV to lower energies with respect to the experiment. As one can see from Fig. 4 and Table II, we observe some shift already in the RRPA calculation, which is determined by the properties of the NL3 forces. Improvement of the forces, for instance, by the use of the density-dependent versions [53,54] of the RMF, should bring the $E1$ mean energy into better agreement with the data.

However, there is an essential difference between the fully self-consistent relativistic calculations of the present work and the nonrelativistic approach. In the nonrelativistic approach discussed in Ref. [38], one introduces on all three stages of the calculation phenomenological parameters, which have to be adjusted to experimental data: first, the Woods-Saxon parameters, for instance, the well depth, are varied to obtain single-particle levels close to the experimental values; second, one of the parameters of the Landau-Migdal force is adjusted to obtain phonon energies at the experimental positions (for each mode); and third, another Landau-Migdal force parameter is varied to reproduce the centroid of the

TABLE II. Lorentz fit parameters in the two energy intervals: B_n–25 MeV and 0–30 MeV, for the $E1$ photoabsorption cross sections in ^{208}Pb and ^{132}Sn, calculated with the RRPA and the RRPA extended to include the particle-phonon coupling (RRPA-PC), compared with data.

		B_n–25 MeV			0–30 MeV		
		$\langle E \rangle$ (MeV)	Γ (MeV)	EWSR (%)	$\langle E \rangle$ (MeV)	Γ (MeV)	EWSR (%)
^{208}Pb	RRPA	13.1	2.4	121	12.9	2.0	128
	RRPA-PC	12.9	4.3	119	13.2	3.0	128
	Exp. [51]	13.4	4.1	117			125(8)
^{132}Sn	RRPA	14.7	3.3	116	14.5	2.6	126
	RRPA-PC	14.4	4.0	112	14.6	3.2	126
	Exp. [52]	16.1(7)	4.7(2.1)	125(32)			

giant resonance. Although the varying of the parameters is performed in relatively narrow limits, it is necessary to obtain realistic results. In contrast, in the relativistic fully consistent approach developed in the present work, no adjustment of additional parameters is made. Of course, the underlying energy functional has been determined in a phenomenological way by a fit to experimental ground state properties of characteristic nuclei. However, it is of universal nature, and the same parameters are used for investigations of many nuclear properties over the entire periodic table. The predictive power of this scheme is therefore much higher than that of the present semiphenomenological approach discussed, for instance, in Ref. [38].

The effect of the particle-vibration coupling on the low-lying dipole strength around the neutron threshold within the presented approach can also be seen in the Figs. 4 and 5. But this phenomenon requires a detailed investigation, which is considered in a special publication [55].

IV. SUMMARY AND OUTLOOK

To describe the damping of collective excitations in nuclei, covariant density functional theory is extended by particle-vibration coupling in a consistent way. Starting from a relativistic energy functional $E[\rho]$, the self-consistent RMF equations are solved and the static part of the nucleon self-energy $\tilde{\Sigma} = \delta E / \delta \rho$ is found. In a second step, the low-lying collective phonons are determined in the framework of relativistic RPA with the effective p-h interaction $\tilde{V} = \delta \tilde{\Sigma} / \delta \rho$. Using particle-phonon vertices deduced from the same interaction, the self-energy $\tilde{\Sigma}$ is extended by an energy-dependent part $\Sigma^e(\varepsilon)$. The Bethe-Salpeter equation derived from the full self-energy $\Sigma = \tilde{\Sigma} + \Sigma^e$ is formulated in the p-h basis of the Dirac eigenstates. Using the time blocking approximation, which allows the truncation to 1p1h⊗phonon configurations, and a subtraction procedure, which avoids double counting of correlations, it is shown that the resulting effective interaction $\tilde{V} + \delta \Phi(\omega)$ contains besides the static part $\tilde{V}$ an energy-dependent correction term $\delta \Phi(\omega)$, which takes into account the coupling of the particles to collective phonons.

This method is applied to the computation of spectroscopic characteristics of nuclear excited states in a wide energy range up to 30 MeV for spherical nuclei with closed shells. An equation for the density matrix variation is formulated and solved in the Dirac space as well in the momentum space. The particle-phonon coupling amplitudes of collective vibrational modes below the neutron separation energy have been calculated within the self-consistent RRPA using the parameter set NL3 for the Lagrangian. The same force has been used for the static part of the effective p-h interaction $\tilde{V}$ and for the evaluation of the particle-phonon vertices $\gamma^\mu_{kk'}$. Therefore a fully consistent description of giant resonances is performed.

Noticeable fragmentation of the isoscalar monopole and isovector dipole giant resonances in ^{208}Pb and ^{132}Sn is obtained due to the particle-vibration coupling. This leads to a significant spreading width as compared to simple RRPA

calculations. This is in agreement with experimental data as well as with the results obtained within the nonrelativistic semiphenomenological approaches of Refs. [33,38].

Thus in the present work, a description of nuclear many-body dynamics including complex configurations is realized within an approach that is (i) fully consistent, (ii) based on relativistic dynamics, (iii) universally valid for nuclei over the entire periodic table, and (iv) based on a modern covariant density functional, which has been applied with great success to many nuclear properties over the entire periodic table.

So far, this extended density functional theory for complex configurations has been formulated only for closed-shell nuclei. To expand the field of applications to nuclei with opened shells, it is, of course, necessary to include pairing correlations in the approach discussed in the present paper. This can be done in the manner of Ref. [37] where pairing correlations and particle-vibration coupling are taken into account on an equal footing in a nonrelativistic framework using techniques of a generalized Green's function formalism. Work in this direction is in progress.

APPENDIX A: NONLINEAR MESON POTENTIALS

So far we started from a Lagrangian [Eq. (1)] containing the nucleons as Dirac particles and mesons providing an interaction between them [46,47], as it is the starting point of most of the relativistic investigations in nuclear physics. It was recognized, however, very early on [56] that this model does not provide an adequate description of the surface properties of realistic nuclei. The incompressibility is too high, and the deformations are too small [7]. Therefore, over the years the relativistic models have been considerably improved by introducing an effective density dependence, in accordance with the concept of density functional theory. Boguta and Bodmer [56] proposed in 1977 to introduce a nonlinear coupling between the σ mesons replacing the mass term $\frac{1}{2} m_\sigma^2 \sigma^2$ in the Lagrangian (1) by a nonlinear meson potential

$$U(\sigma) = \frac{1}{2} m_\sigma^2 \sigma^2 + \frac{g_2}{3} \sigma^3 + \frac{g_3}{4} \sigma^4. \tag{A1}$$

This procedure was used because it did not destroy the renormalizability of the model. In these early days, relativistic models of the nucleus were considered as fully fledged quantum field theories [47], and therefore nonlinear meson

couplings provided an elegant extension of the model containing additional parameters introducing an effective density dependence.

In fact, models with nonlinear meson couplings have been used very extensively in the literature. Very successful parameterizations have been developed on this basis, for instance, NL1 [57] and NL3 [45], which contain only nonlinear couplings between the σ mesons. Later on, one also considered nonlinear couplings between the ω mesons [58,59], however, without improving the agreement between theoretical results and experimental data in finite nuclei. In the present investigations, we consider the parameter set NL3, which has been used with great success for the description of symmetric nuclear matter and finite nuclei with closed shells [7], deformed nuclei, and rotating nuclei [15], and for relativistic RPA calculations of giant resonances and low-lying states [48]. In the most successful applications, pairing correlations are taken into account in the framework of relativistic Hartree-Bogoliubov (RHB) theory with Gogny type interactions in the p-p channel [60]. For a recent review, see Ref. [6].

The effective interaction entering the static part of the nucleon self-energy is in this case given by meson exchange potentials. Without the nonlinear couplings, these interactions are of Yukawa type with a range determined by the mass of the corresponding mesons and with a relativistic structure determined by the quantum numbers of the mesons. In the simplest case of the σ-ω model, we have

$$
\begin{aligned}
\tilde{V}(1,2) &= -g_\sigma^2 D_\sigma(\boldsymbol{r}_1, \boldsymbol{r}_2)\beta^{(1)}\beta^{(2)} \\
&\quad + g_\omega^2 D_\omega(\boldsymbol{r}_1, \boldsymbol{r}_2)(1^{(1)}1^{(2)} - \boldsymbol{\alpha}^{(1)}\boldsymbol{\alpha}^{(2)}) \quad \text{(A2)}
\end{aligned}
$$

with the Dirac matrices β and $\boldsymbol{\alpha}$ and with the propagator in r space

$$
D_m(\boldsymbol{r}_1, \boldsymbol{r}_2) = \frac{1}{4\pi}\frac{e^{-m_m|\boldsymbol{r}_1-\boldsymbol{r}_2|}}{|\boldsymbol{r}_1-\boldsymbol{r}_2|}, \quad \text{for} \quad m = \sigma, \omega. \quad \text{(A3)}
$$

More realistic applications contain in addition a ρ meson and the photon. These potentials are obtained from the Klein-Gordon equations by elimination of the meson degrees of freedom neglecting retardation.

In the nonlinear case, the static Klein-Gordon equation for the σ meson has the form

$$
-\Delta\sigma + U'(\sigma) = -g_\sigma\langle\bar{\psi}\psi\rangle, \quad \text{(A4)}
$$

with

$$
U'(\sigma) = m_\sigma^2\sigma + g_2\sigma^2 + g_3\sigma^3. \quad \text{(A5)}
$$

This is a nonlinear equation, which does not allow for an analytic solution. The numerical solution of Eq. (A4) $\sigma(\boldsymbol{r})$ provides us with the mean field of scalar type

$$
\tilde{\Sigma}_s(\boldsymbol{r}) = g_\sigma\sigma(\boldsymbol{r}). \quad \text{(A6)}
$$

Relativistic RPA is obtained as the small amplitude limit of time-dependent Hartree theory [16]. In this case, the relativistic single-particle density matrix $\rho_{kk'}$ is expanded around the static solution ρ_0. The linearization of the Klein-Gordon

equation (A4) leads to

$$
(-\Delta + M(\boldsymbol{r}))\delta\sigma = -g_\sigma\delta\rho_s, \quad \text{(A7)}
$$

where $\delta\rho_s$ is the scalar density, with $M(\boldsymbol{r})$ depending on the coordinate $\boldsymbol{r}$

$$
M(\boldsymbol{r}) = U''(\sigma_0(\boldsymbol{r})) = m_\sigma^2 + 2g_2\sigma_0(\boldsymbol{r}) + 3g_3\sigma_0^2(\boldsymbol{r}), \quad \text{(A8)}
$$

where $\sigma_0(\boldsymbol{r})$ is the σ field of the static solutions. In momentum space, this leads to a nonlocal propagator, which is the solution of the integral equation

$$
\begin{aligned}
\boldsymbol{q}^2 D_\sigma(\boldsymbol{q}, \boldsymbol{q}') &+ \int \frac{d^3q''}{(2\pi)^3} M(\boldsymbol{q} - \boldsymbol{q}'')D_\sigma(\boldsymbol{q}'', \boldsymbol{q}') \\
&= (2\pi)^3\delta(\boldsymbol{q} - \boldsymbol{q}'), \quad \text{(A9)}
\end{aligned}
$$

where $M(\boldsymbol{q})$ is the Fourier transform of $M(\boldsymbol{r})$:

$$
M(\boldsymbol{q}) = \int d^3r e^{-i\boldsymbol{q}\boldsymbol{r}} M(\boldsymbol{r}). \quad \text{(A10)}
$$

The σ part of the effective p-h interaction used in the RPA calculations has therefore the form

$$
\tilde{V}_\sigma^{ph}(1, 2) = -g_\sigma^2\beta^{(1)}\beta^{(2)} \int \frac{d^3q d^3q'}{(2\pi)^6}e^{i(\boldsymbol{q}\boldsymbol{r}_1-\boldsymbol{q}'\boldsymbol{r}_2)}D_\sigma(\boldsymbol{q}, \boldsymbol{q}')
$$

$$
\text{(A11)}
$$

and similar terms for the other mesons and the photon. We use this interaction in the solution of the relativistic RPA equation for the calculation of the collective phonons, as well as in Eq. (19) for the determination of the corresponding particle-phonon vertices γ_{kl}^μ and in Eq. (36) for the response function $R(14, 23)$.

APPENDIX B: DENSITY-DEPENDENT MESON VERTICES

In recent years, it has been recognized that the relativistic models are by no means fully fledged quantum field theories. Instead, they are effective field theories, which provide the basis of covariant density functional theory. Renormalizability is not important. In the spirit of density functional theory, it is reasonable to abandon the nonlinear couplings and to introduce instead the coupling parameters $g_\sigma(\rho(\boldsymbol{r}))$, $g_\omega(\rho(\boldsymbol{r}))$ and $g_\rho(\rho(\boldsymbol{r}))$, which depend on the baryon density [53,54,61–64].

In this case, the static self-energy contains rearrangement terms, i.e., terms depending on the derivative of the coupling constant with respect to the density. We find

$$
\tilde{\Sigma}_s(\boldsymbol{r}) = g_\sigma\sigma(\boldsymbol{r}). \quad \text{(B1)}
$$

$$
\tilde{\Sigma}_0(\boldsymbol{r}) = g_\omega\omega_0(\boldsymbol{r}) + g_\rho\tau_3\rho_0(\boldsymbol{r}) + V_C(\boldsymbol{r}) + \tilde{\Sigma}^R(\boldsymbol{r}), \quad \text{(B2)}
$$

with the rearrangement term

$$
\begin{aligned}
\tilde{\Sigma}^R(\boldsymbol{r}) &= g_\sigma'(\rho(\boldsymbol{r}))\rho_s(\boldsymbol{r})\sigma(\boldsymbol{r}) + g_\omega'(\rho(\boldsymbol{r}))\rho(\boldsymbol{r})\omega_0(\boldsymbol{r}) \\
&\quad + g_\rho'(\rho(\boldsymbol{r}))\rho_T(\boldsymbol{r})\rho_0(\boldsymbol{r}), \quad \text{(B3)}
\end{aligned}
$$

where $\rho = \rho_p + \rho_n$ and $\rho_T = \rho_p - \rho_n$ are the isoscalar and isovector baryon densities and ρ_0 is the time-like component of the ρ field. Here we have used the fact that we have time-reversal invariance in the ground state and that the currents vanish in this case.

The effective p-h interaction is obtained as the derivative of the self-energy with respect to the density operator. We find for the σ exchange

$$
\begin{aligned}
V_\sigma^{ph}(1,2) \;=\; & -\beta^{(1)}\beta^{(2)}g_\sigma(1)g_\sigma(2)D_\sigma(\boldsymbol{r}_1,\boldsymbol{r}_2) \\
& - I_\sigma(\boldsymbol{r}_1)\delta(\boldsymbol{r}_1-\boldsymbol{r}_2) - \{\beta^{(1)}1^{(2)}g_\sigma(1)\tilde{g}_\sigma(2) \\
& + 1^{(1)}\beta^{(2)}\tilde{g}_\sigma(1)g_\sigma(2) \\
& + 1^{(1)}1^{(2)}\tilde{g}_\sigma(1)\tilde{g}_\sigma(2)\}D_\sigma(\boldsymbol{r}_1,\boldsymbol{r}_2),
\end{aligned} \tag{B4}
$$

with

$$
\begin{aligned}
I_\sigma(\boldsymbol{r}_1) \;=\; & \{(\beta^{(1)}1^{(2)} + 1^{(1)}\beta^{(2)})g_\sigma'(1) + 1^{(1)}1^{(2)}g_\sigma''(1)\rho_s(\boldsymbol{r}_1)\} \\
& \times \int d^3r\, g_\sigma(\rho(\boldsymbol{r}))D_\sigma(\boldsymbol{r}_1,\boldsymbol{r})\rho_s(\boldsymbol{r}),
\end{aligned} \tag{B5}
$$

and similar terms for the ω and ρ exchange. Here we have used the abbreviations

$$
g_\sigma(1) \;:=\; g_\sigma(\rho(\boldsymbol{r}_1)), \tag{B6}
$$

$$
\tilde{g}_\sigma(1) \;:=\; g_\sigma'(\rho(\boldsymbol{r}_1))\rho_s(\boldsymbol{r}_1). \tag{B7}
$$

APPENDIX C: SOLUTION IN MOMENTUM SPACE

First we concentrate on the static interaction $\tilde{V}$ of Eq. (A2), neglecting for the moment the nonlinear meson coupling. We can transform the one-boson exchange (OBE) interaction (A2) to momentum space and neglect retardation:

$$
\tilde{V}(1,2) = \pm\sum_m g_m^2 \int \frac{d^3q}{(2\pi)^3} e^{i\boldsymbol{q}(\boldsymbol{r}_1-\boldsymbol{r}_2)}\Gamma_\mu^m(1)D_m^{\mu\nu}(q)\Gamma_\nu^m(2), \tag{C1}
$$

where the plus sign holds for the vector mesons and the minus sign for the scalar mesons. The index m denotes the set of mesons $m = \{\sigma, \omega, \rho, e\}$, the isoscalar-scalar σ meson, the isoscalar-vector ω meson, the isovector-vector ρ meson, and the photon, which carry the respective components of the interaction. Summation is implied also over the repeated Greek indices. $D_m^{\mu\nu}(q)$ is a boson propagator which is usually taken in the RMF calculations in the simplified Yukawa form neglecting form factors and retardation effects:

$$
D_m(q) \;=\; -\frac{1}{\boldsymbol{q}^2+m_m^2}, \quad m = \sigma, \tag{C2}
$$

$$
D_m^{\mu\nu}(q) \;=\; \frac{g^{\mu\nu}}{\boldsymbol{q}^2+m_m^2}, \quad m = \omega, \rho, e. \tag{C3}
$$

Introducing the channel index $c = (\boldsymbol{q}, m)$, which combines the meson index m with the momentum transfer $\boldsymbol{q}$, we can express

$\tilde{V}$ as a sum of separable terms

$$
\tilde{V}(1,2) = \sum_c d_c Q^{(c)}(1)Q^{(c)\dagger}(2), \tag{C4}
$$

with

$$
Q^{(c)} = Q(\boldsymbol{q}, m) = \Gamma_\mu^m e^{i\boldsymbol{q}\boldsymbol{r}}, \tag{C5}
$$

and the propagator

$$
d_c = d(\boldsymbol{q}, m) = \pm g_m^2 D_m^{\mu\nu}(q). \tag{C6}
$$

The matrix elements of $\tilde{V}$ in Dirac space have the form

$$
\begin{aligned}
\tilde{V}_{k_1k_4,k_2k_3} \;=\; & \langle k_1k_4|\tilde{V}|k_2k_3\rangle = \sum_c d_c Q_{k_1k_2}^{(c)}Q_{k_3k_4}^{(c)*} \\
=\; & \pm\sum_m g_m^2 \int \frac{d^3q}{(2\pi)^3}\langle k_1|\Gamma_\mu^m e^{i\boldsymbol{q}\boldsymbol{r}}|k_2\rangle D_m^{\mu\nu}(q) \\
& \times \langle k_4|\Gamma_\nu^m e^{-i\boldsymbol{q}\boldsymbol{r}}|k_3\rangle.
\end{aligned} \tag{C7}
$$

For nonlinear meson couplings, this expression has to be somewhat modified, because the propagator in momentum space (A11) is nondiagonal in this case. We have $D_m^{\mu\nu}(\boldsymbol{q}, \boldsymbol{q}')$, and the values d_c have to be replaced by matrices $d_{cc'}$ in this case.

APPENDIX D: RESPONSE FORMALISM IN SPHERICAL NUCLEI

In the spherical case, angular momentum coupling reduces the numerical effort considerably. The response equation for $\delta\rho$ reads in this case

$$
\begin{aligned}
\delta\rho_{(k_1k_2)}^J(\omega) \;=\; & \delta\tilde{\rho}_{(k_1k_2)}^J(\omega) + \tilde{R}_{(k_1k_2)}(\omega)\sum_{(k_3k_4)}\big[\tilde{V}_{(k_1k_4,k_2k_3)}^J \\
& + \delta\Phi_{(k_1k_4,k_2k_3)}^J(\omega)\big]\delta\rho_{(k_3k_4)}^J(\omega).
\end{aligned} \tag{D1}
$$

It contains the matrix elements of the static effective interaction $\tilde{V}^J$, and $\delta\Phi^J(\omega)$ is the change of the effective interaction due to the energy dependence of the particle-vibration coupling.

For the meson exchange potentials, we obtain after coupling to good angular momentum J,

$$
\begin{aligned}
\tilde{V}_{(k_1k_4,k_2k_3)}^J \;=\; & \pm\frac{(4\pi)^2}{2J+1}\sum_{LSm}(-1)^S \\
& \times \int_0^\infty \frac{q^2dq}{(2\pi)^3}\langle k_1\|j_L(qr)\big[\Gamma_S^m Y_L\big]^J\|k_2\rangle \\
& \times \frac{g_m^2}{q^2+m_m^2}\langle k_3\|j_L(qr)\big[\Gamma_S^m Y_L\big]^J\|k_4\rangle,
\end{aligned} \tag{D2}
$$

where index $S = (0,1)$ denotes the spherical component of the Pauli matrix entering the vertices (3). The factor $(-)^S$ indicates that the space-like parts of the interaction (current-current interactions) have the opposite sign as the time-like part. The matrix elements [Eq. (D2)] are a sum of separable terms. The dimension of the matrices to be inverted is given by the number of separable terms.

The interaction $\tilde{V}$ is treated in the response equation (72). After transformation of this equation to momentum space, we find

$$
\begin{aligned}
\delta\rho_{LS}^{Jm}(q,\omega) = \ & \delta\rho_{LS}^{(e)Jm}(q;\omega) \\
& \pm \frac{(4\pi)^2}{2J+1}\sum_{L'S'm'}(-1)^{S'}\int_0^\infty \frac{q'^2 dq'}{(2\pi)^3} \\
& \times R_{LS,L'S'}^{(e)Jmm'}(q,q';\omega)\frac{g_{m'}^2}{q'^2+m_{m'}^2}\delta\rho_{L'S'}^{Jm'}(q';\omega),
\end{aligned}
$$
$$(D3)$$

where

$$
\begin{aligned}
R_{LS,L'S'}^{(e)Jmm'}&(q,q';\omega) \\
&= \sum_{(k_1k_2k_3k_4)} Q_{LS(k_1k_2)}^{Jm}(q)R_{(k_1k_4,k_2k_3)}^{(e)J}(\omega)Q_{L'S'(k_3k_4)}^{Jm'}(q'),
\end{aligned}
$$
$$(D4)$$

with

$$
Q_{LS(k_1k_2)}^{Jm}(q) = \langle k_1\|j_L(qr)\left[\Gamma_S^m Y_L\right]^J\|k_2\rangle,
$$
$$(D5)$$

is a Fourier transform of the correlated propagator $R^{(e)J}$ which is determined in the Dirac basis by the angular momentum coupled version of Eq. (66):

$$
\begin{aligned}
R_{(k_1k_4,k_2k_3)}^{(e)J}(\omega) = \ & \tilde{R}_{(k_1k_2)}(\omega)\delta_{(k_1k_3)}\delta_{(k_2k_4)} + \tilde{R}_{(k_1k_2)}(\omega) \\
& \times \sum_{(k_5k_6)}\delta\Phi_{(k_1k_6,k_2k_5)}^{J}(\omega)R_{(k_5k_4,k_6k_3)}^{(e)J}(\omega).
\end{aligned}
$$
$$(D6)$$

The free term on the right side of the Eq. (D3) has the form

$$
\delta\rho_{LS}^{(e)Jm}(q;\omega) = \sum_{(k_1k_2k_3k_4)} Q_{LS(k_1k_2)}^{Jm}(q)R_{(k_1k_4,k_2k_3)}^{(e)}(\omega)P_{(k_3k_4)}^{J},
$$
$$(D7)$$

where

$$
P_{(k_1k_2)}^{J} = \langle k_1\|P^J\|k_2\rangle.
$$
$$(D8)$$

The spectrum of nuclear excitations in the external field P with the multipolarity J is therefore determined by the strength function

$$
S^J(E) = -\frac{1}{\pi}\lim_{\Delta\to+0}\mathrm{Im}\Pi^J(E+i\Delta),
$$
$$(D9)$$

expressed through the polarizability $\Pi^J(\omega)$

$$
\begin{aligned}
\Pi^J(\omega) = \ & \Pi^{(e)J}(\omega) \pm \frac{(4\pi)^2}{2J+1}\sum_{LSm}(-1)^{S} \\
& \times \int_0^\infty \frac{dq q^2}{(2\pi)^3}\delta\rho_{LS}^{(e)Jm}(q;\omega)\frac{g_m^2}{q^2+m_m^2}\delta\rho_{LS}^{Jm}(q;\omega),
\end{aligned}
$$
$$(D10)$$

where

$$
\Pi^{(e)J}(\omega) = \sum_{(k_1k_2k_3k_4)} P_{(k_1k_2)}^{J}R_{(k_1k_4,k_2k_3)}^{(e)J}(\omega)P_{(k_3k_4)}^{J}.
$$
$$(D11)$$

Thus, one can see that it is convenient to solve our problem as well as the RRPA problem in the momentum space, since the rank of vectors and matrices entering Eq. (D3) is determined by the number of mesh points in q space and the number of meson channels. In particular, it does not depend on the mass number of the nucleus. In realistic calculations, the rank of Eq. (D3) in the momentum space is around 500, and obviously the numerical effort does not depend considerably on the total dimension of p-h and α-h subspaces. However, if one stays in the Dirac basis, the latter dimension is exactly the rank of arrays in Eq. (D1). One should keep in mind that in practice, both subspaces are truncated at some energy differences ε_{ph} and $\varepsilon_{\alpha h}$ which are large enough so that a further increase of these values does not influence the results. In light nuclei with relatively small level density, the total dimension of p-h and α-h subspaces is comparable and could be even smaller than the rank of Eq. (D3); therefore, working in the Dirac basis is more preferable. For heavy nuclei, the Dirac basis becomes huge, so using the momentum space is more justified.

However, even if one considers Eq. (D3) in the momentum representation, Eq. (D6) for the correlated propagator, nevertheless, has to be solved in the Dirac basis. This equation contains the particle-phonon coupling amplitude Φ^J with the following matrix elements coupled to angular momentum J:

$$
\begin{aligned}
\Phi_{(ph',hp')}^{J}(\omega) = \sum_\mu \Bigg[& \delta_{(pp')}\frac{\delta_{\varkappa_{h'}\varkappa_h}}{2j_h+1}\sum_{h''}\frac{\gamma_{(h''h)}^{\mu}\gamma_{(h''h')}^{\mu*}}{\omega-\varepsilon_p+\varepsilon_{h''}-\Omega^\mu} \\
& + \delta_{(hh')}\frac{\delta_{\varkappa_{p'}\varkappa_p}}{2j_p+1}\Bigg(\sum_{p''}\frac{\gamma_{(pp'')}^{\mu}\gamma_{(p'p'')}^{\mu*}}{\omega-\varepsilon_{p''}+\varepsilon_h-\Omega^\mu} \\
& + \sum_{\alpha''}\frac{\gamma_{(p\alpha'')}^{\mu}\gamma_{(p'\alpha'')}^{\mu*}}{\omega-\varepsilon_{\alpha''}+\varepsilon_h-\Omega^\mu}\Bigg) + (-1)^{J+J_\mu} \\
& \times \begin{Bmatrix} j_p & j_h & J \\ j_{h'} & j_{p'} & J^\mu \end{Bmatrix}\Bigg(\frac{(-1)^{j_{p'}-j_h}\gamma_{(pp')}^{\mu}\gamma_{(hh')}^{\mu*}}{\omega-\varepsilon_{p'}+\varepsilon_h-\Omega^\mu} \\
& + \frac{(-1)^{j_p-j_{h'}}\gamma_{(p'p)}^{\mu*}\gamma_{(h'h)}^{\mu}}{\omega-\varepsilon_p+\varepsilon_{h'}-\Omega^\mu}\Bigg)\Bigg],
\end{aligned}
$$
$$(D12)$$

where $\varkappa_k$ denotes the relativistic quantum number set: $\varkappa_k = (2j_k+1)(l_k-j_k)$, and $\gamma_{(k_1k_2)}^{\mu} = \langle k_1\|\gamma^\mu\|k_2\rangle$ denotes the reduced matrix element of the particle-phonon coupling amplitude. The backward-going components are found through the symmetry relations

$$
\Phi_{(hp',ph')}^{J}(\omega) = (-1)^{j_h+j_p+j_{h'}+j_{p'}}\Phi_{(p'h,h'p)}^{J}(-\omega).
$$
$$(D13)$$

But this problem is too expensive numerically to be solved in the full Dirac basis. Because of the pole structure of the Φ amplitude, it is natural to suggest that the particle-phonon coupling effect is not quantitatively important far from the Fermi surface. So, in the numerical calculations, an energy window $\varepsilon_{\mathrm{win}}$ was implied around the Fermi surface with respect to p-h energy differences ε_{ph} so that the summation in Eq. (D6) is performed only among the p-h pairs with $\varepsilon_{ph} \leqslant \varepsilon_{\mathrm{win}}$. Consequently, the correlated propagator differs from the mean-field propagator only within this window. This approximation has been investigated numerically by direct

calculations with different values of $\varepsilon_{\mathrm{win}}$, as discussed in Sec. III. It is important to emphasize that many p-h and α-h configurations outside the window are taken into account on the RRPA level, which is necessary in order to obtain the reasonable centroid positions of giant resonances as well as to find the dipole spurious state close to zero energy.

[1] P. Hohenberg and W. Kohn, Phys. Rev. **136**, B864 (1964).

[2] W. Kohn and L. J. Sham, Phys. Rev. **137**, A1697 (1965).

[3] D. Vautherin and D. M. Brink, Phys. Rev. C **5**, 626 (1972).

[4] J. Dechargé and D. Gogny, Phys. Rev. C **21**, 1568 (1980).

[5] P. Ring, Prog. Part. Nucl. Phys. **37**, 193 (1996).

[6] D. Vretenar, A. V. Afanasjev, G. A. Lalazissis, and P. Ring, Phys. Rep. **409**, 101 (2005).

[7] Y. K. Gambhir, P. Ring, and A. Thimet, Ann. Phys. (NY) **198**, 132 (1990).

[8] G. Lalazissis, D. Vretenar, and P. Ring, Eur. Phys. J. A **22**, 37 (2004).

[9] G. A. Lalazissis, M. M. Sharma, P. Ring, and Y. K. Gambhir, Nucl. Phys. **A608**, 202 (1996).

[10] T. Bürvenich, M. Bender, J. A. Maruhn, and P.-G. Reinhard, Phys. Rev. C **69**, 014307 (2004).

[11] J. Meng and P. Ring, Phys. Rev. Lett. **77**, 3963 (1996).

[12] G. A. Lalazissis, D. Vretenar, and P. Ring, Phys. Rev. C **69**, 017301 (2004).

[13] G. A. Lalazissis, D. Vretenar, and P. Ring, Nucl. Phys. **A650**, 133 (1999).

[14] W. Koepf and P. Ring, Nucl. Phys. **A493**, 61 (1989).

[15] A. V. Afanasjev, P. Ring, and J. König, Nucl. Phys. **A676**, 196 (2000).

[16] P. Ring, Z.-Y. Ma, N. Van Giai, D. Vretenar, A. Wandelt, and L.-G. Cao, Nucl. Phys. **A694**, 249 (2001).

[17] N. Paar, P. Ring, T. Nikšić, and D. Vretenar, Phys. Rev. C **67**, 034312 (2003).

[18] N. Paar, T. Nikšić, D. Vretenar, and P. Ring, Phys. Rev. C **69**, 054303 (2004).

[19] A. Ansari, Phys. Lett. **B623**, 37 (2005).

[20] T. Nikšić, D. Vretenar, and P. Ring, Phys. Rev. C **73**, 034308 (2006); **74**, 064309 (2006).

[21] L. D. Landau, Sov. Phys. JETP **8**, 70 (1959).

[22] A. B. Migdal, *Theory of Finite Fermi Systems and Applications to Atomic Nuclei* (Interscience, New York, 1967).

[23] P. Ring and J. Speth, Nucl. Phys. **A235**, 315 (1974).

[24] P. Ring and E. Werner, Nucl. Phys. **A211**, 198 (1973).

[25] I. Hamamoto and P. J. Siemens, Nucl. Phys. **A269**, 199 (1976).

[26] A. Bohr and B. Mottelson, *Nuclear Structure*, Vol. 2 (Benjamin, New York, 1975).

[27] P. F. Bortignon, R. A. Broglia, D. R. Bes, and R. J. Liotta, Phys. Rep. C **30**, 305 (1977).

[28] P. F. Bortignon, R. A. Broglia, D. R. Bes, and C. M. Dasso, Phys. Rep. **120**, 1 (1985).

[29] G. F. Bertsch, P. F. Bortignon, R. A. Broglia, and C. H. Dasso, Phys. Lett. **B80**, 161 (1979).

[30] P. F. Bortignon and R. A. Broglia, Nucl. Phys. **A371**, 405 (1981).

[31] G. Colò, P. F. Bortignon, Nguyen Van Giai, A. Bracco, and R. A. Broglia, Phys. Lett. **B276**, 279 (1992).

[32] G. Colò and P. F. Bortignon, Nucl. Phys. **A696**, 427 (2001).

[33] D. Sarchi, P. F. Bortignon, and G. Colo, Phys. Lett. **B601**, 27 (2004).

[34] V. I. Tselyaev, Yad. Fiz. **50**, 1252 (1989) [Sov. J. Nucl. Phys. **50**, 780 (1989)].

[35] S. P. Kamerdzhiev, G. Ya. Tertychny, and V. I. Tselyaev, Phys. Part. Nucl. **28**, 134 (1997).

[36] S. P. Kamerdzhiev, J. Speth, and G. Tertychny, Phys. Rep. **393**, 1 (2004).

[37] V. I. Tselyaev, Phys. Rev. C **75**, 024306 (2007).

[38] E. V. Litvinova and V. I. Tselyaev, Phys. Rev. C **75**, 054318 (2007).

[39] V. G. Soloviev, *Theory of Atomic Nuclei: Quasiparticles and Phonons* (Institute of Physics, Philadelphia, 1992).

[40] S. Drożdż, S. Nishizaki, J. Speth, and J. Wambach, Phys. Rep. **197**, 1 (1990).

[41] V. A. Khodel and E. E. Saperstein, Nucl. Phys. **A317**, 424 (1979).

[42] V. A. Khodel and E. E. Saperstein, Nucl. Phys. **A348**, 261 (1980).

[43] S. A. Fayans, S. V. Tolokonnikov, E. L. Trykov, and D. Zawischa, Nucl. Phys. **A676**, 49 (2000).

[44] E. Litvinova and P. Ring, Phys. Rev. C **73**, 044328 (2006).

[45] G. A. Lalazissis, J. König, and P. Ring, Phys. Rev. C **55**, 540 (1997).

[46] J. D. Walecka, Ann. Phys. (NY) **83**, 491 (1974).

[47] B. D. Serot and J. D. Walecka, Adv. Nucl. Phys. **16**, 1 (1986).

[48] Z.-Y. Ma, A. Wandelt, N. Van Giai, D. Vretenar, P. Ring, and L.-G. Cao, Nucl. Phys. **A703**, 222 (2002).

[49] P. Ring and P. Schuck, *The Nuclear Many-Body Problem* (Springer-Verlag, New York, 1980).

[50] S. Shlomo and D. H. Youngblood, Phys. Rev. C **47**, 529 (1993).

[51] A. Veyssiere, H. Beil, R. Bergere, P. Carlos, and A. Lepretre, Nucl. Phys. **A159**, 561 (1970).

[52] P. Adrich, A. Klimkewicz, M. Fallot *et al.*, Phys. Rev. Lett. **95**, 132501 (2005).

[53] T. Nikšić, D. Vretenar, P. Finelli, and P. Ring, Phys. Rev. C **66**, 024306 (2002).

[54] G. A. Lalazissis, T. Nikšić, D. Vretenar, and P. Ring, Phys. Rev. C **71**, 024312 (2005).

[55] E. Litvinova, P. Ring, and D. Vretenar, Phys. Lett. **B647**, 111 (2007).

[56] J. Boguta and A. R. Bodmer, Nucl. Phys. **A292**, 413 (1977).

[57] P. G. Reinhard, M. Rufa, J. Maruhn, W. Greiner, and J. Friedrich, Z. Phys. A **323**, 13 (1986).

[58] A. R. Bodmer, Nucl. Phys. **A526**, 703 (1991).

[59] Y. Sugahara and H. Toki, Nucl. Phys. **A579**, 557 (1994).

[60] T. Gonzales-Llarena, J. L. Egido, G. A. Lalazissis, and P. Ring, Phys. Lett. **B379**, 13 (1996).

[61] R. Brockmann and H. Toki, Phys. Rev. Lett. **68**, 3408 (1992).

[62] C. Fuchs and H. Lenske, Phys. Lett. **B345**, 355 (1995).

[63] C. Fuchs, H. Lenske, and H. H. Wolter, Phys. Rev. C **52**, 3043 (1995).

[64] S. Typel and H. H. Wolter, Nucl. Phys. **A656**, 331 (1999).